

# NATIONAL AIR INTELLIGENCE CENTER



MEASUREMENT AND ANALYSIS OF PROPERTIES OF SEVERAL TYPES  
OF FILMS DOPED WITH OXIDES

by

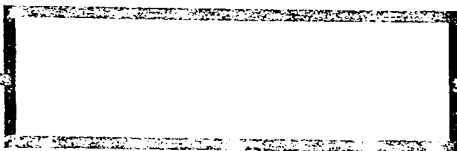
Chen Yuming, Tang Jinfa, Gu Peifu



DTIC QUALITY INSPECTED 5

19950512 057

Approved for public release;  
Distribution unlimited.



**HUMAN TRANSLATION**

NAIC-ID(RS)T-0757-94 5 April 1995

MICROFICHE NR: 95000158

MEASUREMENT AND ANALYSIS OF PROPERTIES OF SEVERAL TYPES  
OF FILMS DOPED WITH OXIDES

By: Chen Yuming, Tang Jinfa, Gu Peifu

English pages: 12

Source: Guangxue Xuebao, Vol. 6, Nr. 1, January 1986;  
pp. 70-75

Country of origin: China

Translated by: SCITRAN  
F33657-84-D-0165

Requester: NAIC/TATD/Bruce Armstrong

Approved for public release; Distribution unlimited.

THIS TRANSLATION IS A RENDITION OF THE ORIGINAL FOREIGN TEXT WITHOUT ANY ANALYTICAL OR EDITORIAL COMMENT STATEMENTS OR THEORIES ADVOCATED OR IMPLIED ARE THOSE OF THE SOURCE AND DO NOT NECESSARILY REFLECT THE POSITION OR OPINION OF THE NATIONAL AIR INTELLIGENCE CENTER.

PREPARED BY:

TRANSLATION SERVICES  
NATIONAL AIR INTELLIGENCE CENTER  
WPAFB, OHIO

GRAPHICS DISCLAIMER

All figures, graphics, tables, equations, etc. merged into this translation were extracted from the best quality copy available.

Accession For	
NTIS CRA&I	<input checked="" type="checkbox"/>
DTIC TAB	<input type="checkbox"/>
Unannounced	<input type="checkbox"/>
Justification .....	
By .....	
Distribution /	
Availability Codes	
Dist	Avail and/or Special
A-1	

MEASUREMENT AND ANALYSIS OF PROPERTIES OF SEVERAL TYPES OF FILMS  
DOPED WITH OXIDES

/70\*

Chen Yuming Tang Jinfu Gu Peifu

ABSTRACT

This article introduces several types of experimental equipment associated with the measurement of stress, absorption, and scattering in thin films. It makes use of these systems to carry out measurements and tests on such characteristics as stress, absorption, scattering, focusing density, and so on, in a number of common oxides and their doping films. At the same time, with the help of Auger energy spectra techniques and X-ray diffraction technology, it analyzes the chemical constituents and crystal structure of films, obtaining a number of significant results.

I. INTRODUCTION

Making use of thin film doping techniques, it is possible to improve the optical and mechanical properties of thin films, obtaining new film materials. For example, Fujiwara [1], in zinc sulfide, doped in cerium fluoride, after which, there was caused a very great increase in the degree of firmness associated with the thin films. Moreover, with the doping of cerium oxide into certain oxide compounds, it is then possible to promote the oxide functions reducing membrane layer absorption and lowering the degree of evaporation difficulty [2]. Pulker and Maser [3,4] did research on the effects of doping vis a vis film stress. Into magnesium fluoride, they doped small amounts of calcium fluoride and zinc fluoride, causing stress associated with  $MgF_2$  to be reduced by half. The studies of Pellicori [5] also clearly show that the doping into cerium fluoride films of other fluorides is followed by the possibility of very great changes in the

---

\* Numbers in margins indicate foreign pagination.  
Commas in numbers indicate decimals.

appearance of their mechanical properties. Besides this, after going through the doping of thin films, the crystal structures and so on also possess possibilities superior to those of thin films that have not been doped. Sanders et al [6] doped into zirconium oxide different proportions of magnesium oxide and silicon oxide. Making use of conventional heat evaporation techniques, they obtained amorphous films with compact structures.

With regard to the key effects given rise to by the improved optical and mechanical properties of doped thin films, we carried out measurements and analysis of properties associated with a number of doped oxide films. We set up a "cat eye" interference system capable of real time stress measurements within thin films. We did real time measurements of stress changes within thin silicon oxide, zirconium oxide, and titanium oxide films and did test measurements. With regard to such properties as absorption, scattering, concentration densities, and so on, associated with thin films, respective use was made of attenuation full reflection methods [7], integrating sphere methods [8], and crystalline vibration methods [9] to carry out measurements. Finally, measurements and analyses were carried out on the crystal structures, chemical constituents, and so on, associated with a number of dope films.

## II. EXPERIMENTAL MEASUREMENT EQUIPMENT

### 1. Thin Film Stress Measurement

We made use of a "cat eye" interferometer installed in a vacuum film plating device in order to measure amounts of substrate deformation during thin film deposition processes. This equipment--compared to ordinary thin film stress interferometers--possesses the special characteristics [10] of vibration resistance and resistance to thermal perturbations.

The "cat eye" interference system installed in a DMD-450 multilayer film plating device is as shown in Fig.1. The polarized laser light  $p$  put out by the polarized He-Ne laser passes through the beam expander, and, after it is expanded, it goes through a polarizing prism and a  $1/4$  wave plate. The wave plate fast axis forms a  $45^\circ$  angle with the vibration direction of the  $p$  polarized light. After light beams enter the vacuum chamber, they are incident on the "cat eye" lens. The function of the "cat eye" lens is to take incident parallel light rays and focus them on the back surface (the back surface is plated with a beam splitting film). Right next to the back surface of the "cat eye" lens is placed a very thin piece of test measurement substrate with a metal film plated on its upper surface (0.15 - 0.5mm thick glass or fused quartz). In this way, the two beams of light reflected from the back surface of the "cat eye" lens and the upper surface of the substrate will then give rise to interference. Interference light beams pass through the  $1/4$  wave plate. After that, the polarization direction relative to incident light is rotated  $90^\circ$ . After arriving at the polarization lens, there is almost complete reflection. At this time, in the reflected light, it is possible to see Newtonian interference band patterns of a similar form. During processes of thin film deposition--due to the existence of thin film stresses--there will be caused the occurrence of substrate deformations. At this time, interference band patterns will then contract (corresponding to compression stress) or expand (corresponding to extension stress). If, in interference fields, one places receivers to measure the band change number  $N$ , it is then possible, from the equation below, to calculate the amount of substrate deformation  $W$ :

$$W = N(\lambda_0/2), \quad (1)$$

In the equation,  $\lambda_0$  is the laser light wavelength.

Going a step further, from the equation below, one obtains stresses within thin films [10]

$$S = \frac{4EW}{3(1-\nu)} \left(\frac{h}{D}\right)^2 \frac{1}{d}, \quad (2)$$

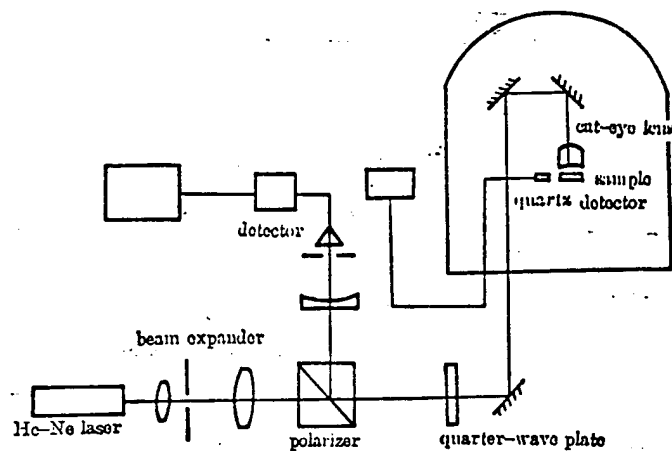


Fig.1 Experimental set up for measuring stress in a thin film

In the equation,  $E$  and  $\nu$  are substrate Young moduli and Poisson ratios.  $h$  is substrate thickness.  $D$  is substrate diameter.  $d$  is film thickness.

We used quartz crystal oscillators to measure changes in the oscillation frequencies of quartz sheets during evaporation processes, thus accurately specifying the thickness  $d$  of thin evaporation films.

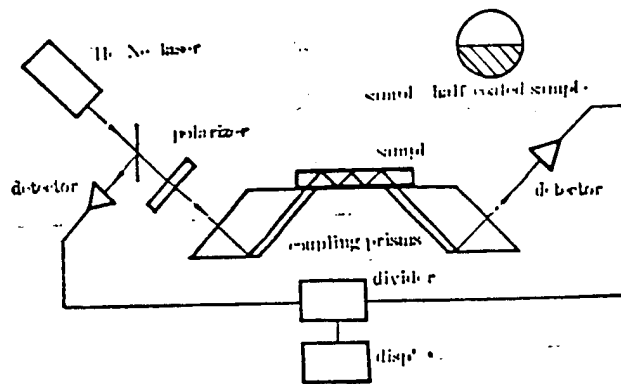


Fig.2 Setup for determining absorption of a thin film

## 2. Measurements of Weak Thin Film Absorption

Use was made of attenuation full reflection methods to measure weak absorption associated with thin films [7]. Experimental equipment was as shown in Fig.2. Light beams pass through prisms and are coupled into glass samples. After going through numerous iterations of interior reflection associated with film plated surfaces, checking measurements are done by detectors. Test measurement samples are half film plated. First of all, light beams are taken and coupled into sections which have not been film plated, obtaining light beam strength  $I_0$ . Following this, samples are shifted, taking light beams and coupling them into film plated sections, obtaining  $I_1$ . Then the attenuation full reflection rate is

$$R = \sqrt[m]{(I_1/I_0)}, \quad (3)$$

In the equation,  $m$  is the number of iterations of reflection of light beams inside samples. The measurements described above were carried out respectively on  $p$  polarization and  $s$  polarization light. Going through inversion, it is then possible

to obtain dulling coefficients  $k$  and thicknesses  $d$ .

### 3. Measurements of Thin Film Relative Scattering

Relative scattering measurements were carried out on equipment [8] shown in Fig.3. Measurement steps were:

- (1) First of all, measure background signal  $I_a$ . /72
- (2) Take sample, place it at the center of the integrating sphere, and measure scattering signal  $I_B$ .
- (3) Move the sample out to determine scattering signal  $I_C$  associated with standard scattering sheets.

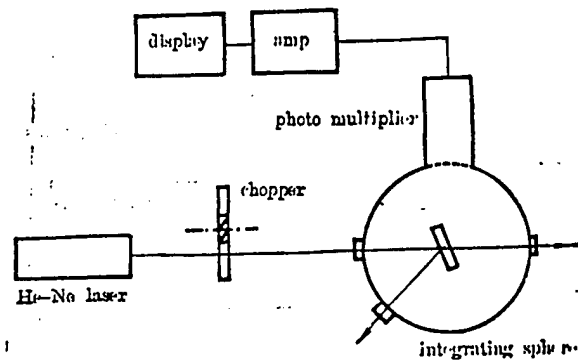


Fig.3 Setup for determining scattering of a thin film

Following that, calculate relative scattering rates from the equation below

$$S = (I_B - I_A)\eta / I_C, \quad (4)$$

In the equation,  $\eta$  is the scattering rate associated with standard scattering sheets. This is one type of relative measurement method for scattering rates. The degree of accuracy of test measurements depends to a very great extent on scattering sheets. However, the experimental data is capable of supplying

relative comparisons.

#### 4. Thin Film Concentration Density Measurements

With regard to thin film concentration densities, it is possible to use a quartz crystal probe installed in a film plating device to measure oscillation frequencies  $f_0$  before film plating, frequencies  $f_1$  after film plating, as well as frequencies  $f'_1$  after vacuum chambers have been filled with moist air. Then, thin film concentration densities can be calculated from the equation below

$$\rho = (f_1 - f_0) / [f_1 - f_0 + \rho_1(f'_1 - f_1)], \quad (5)$$

In the equation,  $\rho_1$  is the density of large pieces of material.

### III. EXPERIMENTAL RESULTS

Making use of the experimental equipment described above, we carried out test measurements of such properties as stress, absorption, scattering, concentration density, and so on, associated with  $\text{SiO}_2$ ,  $\text{ZrO}_2$ , and  $\text{TiO}_2$  thin films as well as their doped films. Experimental samples were manufactured in a DMD-450 multilayer film plating device. Doped thin film materials were hot pressed pieces of material supplied by the Beijing general non-ferrous metals research institute. With regard to the cold substrate deposition of thin films, the measured stress values included thermal stresses given rise to by differences in film layer and substrate coefficients of expansion. However, in the case of hot substrate thin film deposition, due to the fact that, during measurements, substrate temperatures are basically

maintained constant, the stress values obtained in measurements are, therefore, principally intrinsic stresses.

TABLE 1. EXPERIMENTAL RESULTS OF SiO<sub>2</sub> AND SCHOTT-8329 FILMS

material	thickness (Å)	stress (kg/cm <sup>2</sup> )	absorption <i>k</i>	scattering		concentration density
				film (substrate)	substrate	
SiO <sub>2</sub>	2150	+280	2.9×10 <sup>-4</sup>	1.41×10 <sup>-3</sup>	1.375×10 <sup>-3</sup>	0.78
	2000	-690	4.1×10 <sup>-4</sup>	1.1×10 <sup>-3</sup>	1.0×10 <sup>-3</sup>	0.91*
Schott- 8329	1840	+450	5.2×10 <sup>-4</sup>	1.55×10 <sup>-3</sup>	1.47×10 <sup>-3</sup>	0.94
	2443	+300	8.25×10 <sup>-4</sup>	5.1×10 <sup>-4</sup>	4.8×10 <sup>-4</sup>	0.95*

Note: "\*" indicates deposition on hot substrate ( $T_s=200^\circ\text{C}$ ).

Others refer to deposition at room temperature. "+" indicates extension stress; "-" indicates compression stress.

The refractive indices of Schott-8329 glass films deposited on the cold and hot substrates are 1.47 and 1.49, respectively.

/73

Table 1 is test measurement results associated with SiO<sub>2</sub> and Schott-8329 glass thin films. From Table 1, it is possible to see that concentration densities associated with thin Schott-8329 glass films are very much higher than concentration densities associated with SiO<sub>2</sub>. As far as stresses being extension stresses is concerned, in numerical values, they are somewhat larger than SiO<sub>2</sub> films. Scattering are quite close to SiO<sub>2</sub>. However, absorptions show some increases. Schott-8329 glass is glass of which a very small amount is capable of acting as initial thin film material. Making use of Auger energy spectrum instruments, analyses were carried out of the chemical constituents of Schott-8329 glass thin films (Fig.4). It was discovered that the main constituent is SiO<sub>2</sub>. However, it contains certain trace elements. With regard to comprehensive analysis of optical spectra test results, these trace elements were specified as B, Al, and Na. Because of this, Schott-8329 glass can be recognized as being small amounts of the doping oxides B<sub>2</sub>O<sub>3</sub>, Al<sub>2</sub>O<sub>3</sub>, and Na<sub>2</sub>O added into SiO<sub>2</sub>. X-ray diffraction

graphs clearly show that thin films associated with this type of material composition present amorphous structures as shown in Fig.5.

Fig.4 AES spectrum of a Schott-8329 glass film

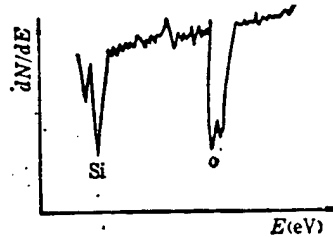
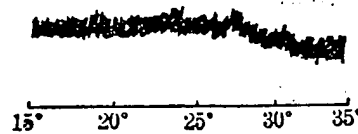


Fig.5 X-ray diffraction analysis of a Schott-8329 glass film



Experimental results associated with  $TiO_2$  and its doped films as well as  $ZrO_2$  and its doped films are respectively set out in Table 2. It is possible to discover that concentration densities associated with  $ZrO_2$  and  $TiO_2$  films after doping are all very greatly raised. Doped films associated with cold substrate deposition have concentration densities which can be higher than nondoped films associated with hot substrate /74 deposition.  $TiO_2$  thin film stresses after doping are increased to some extent. However,  $ZrO_2$  thin film stresses after the addition of MgO are somewhat reduced. Doping is capable of altering thin film stresses. However, due to the fact that there are relationships between thin film stresses and micro structures as well as cylindrical surface energies and other similar factors, the result is that relationships are relatively

complicated. Up to the present time, a consistent understanding has not been arrived at. After doping, thin film absorption shows obvious reductions. Speaking in terms of  $ZrO_2$  films doped with  $Y_2O_3$ , this phenomenon is particularly clear.

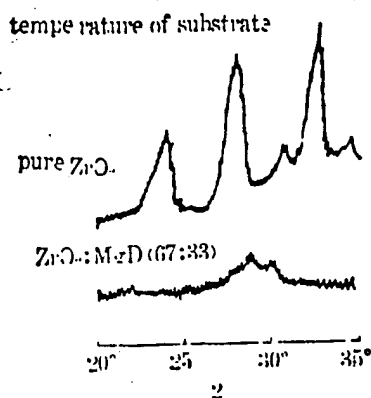
TABLE 2. COMPARISON OF PROPERTIES BETWEEN  $TiO_2$  AND  $TiO_2$  DOPED FILMS,  $ZrO_2$  AND  $ZrO_2$  DOPED FILMS

material	stress (kg/cm <sup>2</sup> )	refractive index	absorption	scattering		concentration density
				film (substrate)	substrate	
$TiO_2$	+700	1.90	$3.2 \times 10^{-3}$	$3.22 \times 10^{-3}$	$2.2 \times 10^{-3}$	0.72
	-310	2.11	$4.1 \times 10^{-3}$	$2.1 \times 10^{-3}$	$1.05 \times 10^{-3}$	0.92*
$TiO_2:MgO$ (54:46)	+1880	1.82	$6.38 \times 10^{-4}$	$8.66 \times 10^{-4}$	$7.46 \times 10^{-4}$	0.95
	+1000	1.91	$9.3 \times 10^{-4}$	$9.5 \times 10^{-4}$	$7.8 \times 10^{-4}$	0.96*
$TiO_2:MgO$ (82:18)	+1750	1.81	$1.5 \times 10^{-3}$	$5.7 \times 10^{-4}$	$4.9 \times 10^{-4}$	0.92
	+1140	1.94	$1.8 \times 10^{-3}$	$8.11 \times 10^{-4}$	$7.2 \times 10^{-4}$	0.92*
$ZrO_2$	+1300	1.78	$1.56 \times 10^{-3}$	$1.1 \times 10^{-3}$	$5.3 \times 10^{-4}$	0.65
	+1030	1.92	$2.09 \times 10^{-3}$	$1.35 \times 10^{-3}$	$9.76 \times 10^{-4}$	0.86*
$ZrO_2:MgO$ (67:33)	+1160	1.70	$5.32 \times 10^{-4}$	$9.5 \times 10^{-4}$	$6.8 \times 10^{-4}$	0.90
	+1040	1.81	$1.55 \times 10^{-3}$	$9.3 \times 10^{-4}$	$6.3 \times 10^{-4}$	0.93*
$ZrO_2:MgO$ (51:49)	+800	1.67	$6.1 \times 10^{-4}$	$9.0 \times 10^{-4}$	$7.8 \times 10^{-4}$	0.93
	+300	1.84	$7.2 \times 10^{-4}$	$1.44 \times 10^{-3}$	$8.5 \times 10^{-4}$	0.95*
$ZrO_2:Y_2O_3$ (79:21)	+1876	1.80	$5.6 \times 10^{-4}$	$1.1 \times 10^{-3}$	$5.9 \times 10^{-4}$	0.89
	+1060	1.82	$7.72 \times 10^{-4}$	$1.38 \times 10^{-3}$	$1.04 \times 10^{-3}$	0.95*
$ZrO_2:Y_2O_3$ (92:8)	+1865	1.81	$6.0 \times 10^{-4}$	$9.9 \times 10^{-4}$	$9.5 \times 10^{-4}$	0.87
	+1200	1.85	$5.5 \times 10^{-4}$	$8.5 \times 10^{-4}$	$5.9 \times 10^{-4}$	0.90*

Note: Thickness of film is about  $1000\text{\AA}$ ;

The weight ratio of raw materials is taken as the dopant ratio.

Fig.6 X-ray diffraction analysis of  $ZrO_2$  and  $ZrO_2$ -doped film



We used X-ray diffraction technology to analyze the crystal structures of  $ZrO_2$  thin films after doping with MgO as shown in Fig.6.  $ZrO_2$  films associated with hot substrate deposition show a polycrystalline form. However, after doping with MgO, the crystal structure has already turned into an amorphous state.

#### IV. CONCLUSIONS

From the experimental results described above, it is possible to obtain the following conclusions:

(1) Concentration densities of thin films after doping show relatively large increases.

(2) Absorptions associated with oxide doped thin films are smaller than nondoped thin films. It is possible to imagine that the sizes of doping molecules and main body molecules are different. When they form thin films, small particle molecules are capable of filling in the gaps in large particle molecules. The result is to raise the concentration densities of thin films. At the same time, the adding in of oxides reduces the dissociation of high valence oxides, promoting oxide function. Going a step further, thin film absorption is reduced.

Obviously, increases in doped thin film concentration densities and absorption reductions are significant with regard to reducing thin film optical instability and raising thin film resistance to laser damage.

Comrade Jin Shangzhong assisted in determining thin film absorptions. The physics department surface physics laboratory and the school central laboratory carried out sample Auger energy spectrum analyses and X-ray diffraction analyses. For this, we all wish to express our thanks.

#### REFERENCES

- [1] S. Fujiwara; *J. Opt. Soc. Am.*, 1963, **53**, No. 11 (Nov), 1317.
- [2] H. A. 麦克劳德;《光学薄膜技术》, (国防工业出版社, 1969), 379.
- [3] H. K. Pulker; *Thin Solid Films*, 1979, **58**, No. 2 (Apr), 371.
- [4] H. K. Pulker, J. Mäser; *Thin Solid Films*, 1979, **59**, No. 1 (Apr), 65.
- [5] S. F. Pellicori; *Thin Solid Films*, 1984, **113**, No. 4 (Mar), 287.
- [6] D. M. Sanders *et al.*; *Proc. SPIE*, 1982, **346**, (Arlington, Virginia), 31.
- [7] 金尚忠, 唐晋发, 吴启宏;《浙江大学学报》, 待发表。
- [8] 刘化文;私人通讯, 1981.
- [9] 顾培夫;《浙江大学学报》, 1982, No. 4 (Dec), 47.
- [10] A. M. Ledger, R. C. Bastien; *Technical Report, Contract DAA25-76-0410 (DAEPA)*, Perkin-Elmer Corp., Norwalk, Conn., 1977 (Jun).

DISTRIBUTION LIST

DISTRIBUTION DIRECT TO RECIPIENT

<u>ORGANIZATION</u>	<u>MICROFICHE</u>
B085 DIA/RIS-2FI	1
C509 BALLOC509 BALLISTIC RES LAB	1
C510 R&T LABS/AVEADCOM	1
C513 ARRADCOM	1
C535 AVRADCOM/TSARCOM	1
C539 TRASANA	1
Q592 FSTC	4
Q619 MSIC REDSTONE	1
Q008 NTIC	1
Q043 AFMIC-IS	1
E051 HQ USAF/INET	1
E404 AEDC/DOF	1
E408 AFWL	1
E410 AFDTC/IN	1
E429 SD/IND	1
P005 DOE/ISA/DDI	1
P050 CIA/OCR/ADD/SD	2
1051 AFIT/LDE	1
PO90 NSA/CDB	1
2206 FSL	1

Microfiche Nbr: FTD95C000158  
NAIC-ID(RS)T-0757-94